DALTON
FULL PAPER

Synthesis and characterisation of trialkylaluminium–dialkylamine adducts: X-ray diffraction and ^{1}H NMR studies†

Donald C. Bradley,* Gregory Coumbarides, Ian S. Harding, Geoffrey E. Hawkes, Izaque A. Maia and Majid Motevalli

Department of Chemistry, Queen Mary & Westfield College, Mile End Road, London, UK E1 4NS

Received 14th April 1999, Accepted 23rd August 1999

Trialkylaluminium–dialkylamine adducts of general formula $R^1{}_3Al{\cdot}NHR^2{}_2$ (R^1 = Me, Et, Pr^i, Bu^i or Bu^t; R^2 = Me, Et, Pr^i or Bu^i) were synthesized by reacting $R^1{}_3Al$ and $NHR^2{}_2$. at high temperatures these adducts either eliminate alkane, forming dimeric amides, or dissociate. Increase in the bulk of R^1 favours alkane elimination. In the ^{1}H NMR spectra of the complexes $R^1{}_3Al{\cdot}NHEt_2$ the methylene protons of the ethyl groups exhibited non-equivalence, and the high-temperature coalescence of the methylene proton signals is due to exchange processes involving both the breaking and reforming of the Al–N dative bond, in a unimolecular or a bimolecular step. The free energy of activation for this process has been correlated to the bulk of the groups R^1. The crystal structures of $Me_3Al{\cdot}NHMe_2$ and $Bu^t{}_3Al{\cdot}NHEt_2$ were determined and their molecular structures are discussed.

Introduction

The compounds $R^1{}_3Al{\cdot}NHR^2{}_2$ are, like other alkylaluminium adducts,[1,2] monomeric crystalline solids or colourless liquids of 1 : 1 stoichiometry. They are commonly synthesized by the exothermic reaction between the Lewis acid ($R^1{}_3Al$) and the base ($NHR^2{}_2$) as in reaction (1), but in solution or as neat liquids

$$R^1{}_3Al + HNR^2{}_2 \rightleftharpoons R^1{}_3Al{\cdot}NHR^2{}_2 \qquad (1)$$

they may partially dissociate. The equilibrium is influenced by the steric and electronic effects of the substituents R^1 and R^2 because they modify the strength of the Al–N dative bond: those which decrease the electron density at aluminium and increase it at nitrogen produce a stronger adduct Al–N bond.

The adducts may also undergo further reaction. In the presence of a second base dissociation (reverse of reaction (1)) facilitates amine exchange, reaction (2).

$$R^1{}_3Al{\cdot}NHR^2{}_2 + R_2NH \longrightarrow R^1{}_3Al{\cdot}NHR_2 + R^2{}_2NH \qquad (2)$$

More recent work[3] has shown that other groups around the metal can also undergo exchange; $EtH_2Al{\cdot}NMe_3$ and $Et_2HAl{\cdot}NMe_3$ are fluxional mixtures of all $Et_xH_{3-x}Al{\cdot}NMe_3$ (x = 0 to 3) species both neat and in aromatic solvents. The adducts may also be subject to irreversible alkane elimination upon heating as in reaction (3). Here the adduct eliminates an alkane

$$2\,R^1{}_3Al{\cdot}NHR^2{}_2 \longrightarrow (R^1{}_2AlNR^2{}_2)_2 + 2\,R^1H \qquad (3)$$

molecule to give a dimeric dialkylaluminium dialkylamide, which is a direct consequence of the N*H* acidity and the Al–*C* carbanion character. In the cases where all R^1 substituents are alkyl groups the N*H* acidity prevails as the controlling factor. In the cases where one of the R^1 groups is substituted by a halogen atom, however, the controlling factor has been attributed to the Al–C bond polarity.[4] The minor role played by N*H* proton acidity in the elimination of alkane is also supported by studies with complexes $AlEt_{(3-x)}Cl_x{\cdot}D$ (D = NH_3, NH_2Me or NH_2Ph) where increasing substitution of Et and Cl led to greater stability of the complex due to the inductive effect of the chlorine despite the increasing acidity of the N*H* proton.[5] A broader-based mechanism for the elimination reaction has been proposed which considers the electronic and steric factors in the whole molecule;[6] a mechanism which was based on the observation that the elimination is autocatalysed by the product, an amide in the monomeric form. This debate continues with the suggestion that amide formation is the result of interaction between a dissociated aluminium trialkyl and an adduct molecule.[7]

In this work we therefore focus our attention on the effects of the R^1 and R^2 groups in the complexes $R^1{}_3Al{\cdot}NHR^2{}_2$ with regard to their stability towards dissociation in solution. The trialkylaluminium–dialkylamine adducts, $R^1{}_3Al{\cdot}NHR^2{}_2$ (R^1 = Me, Et, Pr^i, Bu^i or Bu^t; R^2 = Me, Et, Pr^i or Bu^i), were synthesized by treating the trialkylaluminium (Lewis acceptor) with the dialkylamine (Lewis donor). The numbering scheme for these compounds is shown in Table 1.

Results and discussion

Infrared spectra

The N–H stretching peaks of the adducts are all sharp, indicating that no hydrogen bonding is taking place.[8] From the frequencies listed in Table 1 it is clear that adduct formation always results in a decrease in the frequency of ν_{N-H} compared to that of the free amine, which is in accord with observations on the more limited series of adducts $Me_3Al{\cdot}NHR^2{}_2$ (R^2 = Et, Pr^n, Pr^i, Bu^n or Bu^i).[9] Since coupling of other vibrations with this mode will be insignificant, a reduction in the force constant for ν_{N-H} is indicated. This apparent weakening of the N–H bond may be attributed to a change in s character upon co-ordination of the amine to aluminium. A trend in this general weakening is apparent for adducts with the same amine, as the bulk of the alkyl groups on aluminium increases. With only two significant exceptions ($Pr^i{}_3Al{\cdot}NHBu^i{}_2$ and $Et_3Al{\cdot}NHPr^i{}_2$) the stretching frequency rises then falls with increasing bulk of the metal–alkyl group. This indicates that the weakening of the N–H bond is most severe when the alkylaluminium groups are either very small or very large. This mirrors the rise and then

† *Supplementary data available*: preparative details and characterisation data. For direct electronic access see http://www.rsc.org/suppdata/dt/1999/3553/, otherwise available from BLDSC (No. SUP 57633, 11 pp.). See Instructions for Authors, 1999, Issue 1 (http://www.rsc.org/dalton).

Table 1 Selected infrared[a] and mass spectral data for the adducts $R^1{}_3Al{\cdot}NHR^2{}_2$

			Infrared spectroscopy					Mass spectra	
R^2	R^1	Compound	ν_{N-H}	Frequencies associated with the adduct core				M^+-R	Intensity (%)
Me	Me	**1**	3241 (m)	708 (br, s)	622 (sh, m)	593 (sh, w)	523 (m)	M^+-Me	100
(3368w)[b]	Et	**2**	3282 (m)	638 (br, vs)	571 (sh, vs)	—	497 (m)	Dissoc.[c]	
	Bu^i	**3**	3286 (m)	682 (br, vs)	670 (sh, vs)	595 (m)	530 (s)	M^+-Bu^i	78
	Pr^i	**4**	3278 (vs)	600 (br, vs)	575 (sh, vs)	497 (vs)	423 (s)	M^+-Pr^i	50
	Bu^t	**5**	3265 (m)	565 (s)	470 (s)	448 (sh, w)	425 (m)	Dissoc.[c]	
Et	Me	**6**	3249 (s)	703 (br, vs)	627 (sh, vs)	582 (sh, w)	524 (m)	M^+-Et	56
(3290m)[b]	Et	**7**	3258 (w)	638 (br, s)	—	—	—	M^+-Et	56
	Bu^i	**8**	3264 (w)	677 (br, s)	—	—	—	Dimer[d]	
	Pr^i	**9**	3259 (m)	596 (br, vs)	—	429 (w)	426 (s)	Dissoc.[c]	
	Bu^t	**10**	3249 (m)	586 (m)	559 (s)	—	424 (s)	Dissoc.[c]	
Bu^i	Me	**11**	3246 (m)	703 (br, vs)	625 (s)	577 (sh, w)	525 (m)	M^+-Me	100
(absent)[b]	Et	**12**	3283 (m)	648 (br, vs)	620 (sh, s)	—	495 (m)	M^+-Et	100
	Bu^i	**13**	3285 (w)	677 (br, vs)	—	—	430 (m)	M^+-Bu^i	60
	Pr^i	**14**	3200 (m)	595 (br, vs)	—	493 (m)	431 (vs)	Dissoc.[c]	
	Bu^t	**15**	3265 (w)	597 (w)	561 (m)	—	420 (m)	Dissoc.[c]	
Pr^i	Me	**16**	3238 (m)	703 (br, vs)	639 (m)	582 (w)	527 (m)	Dissoc.[c]	
(absent)[b]	Et	**17**	3225 (w)	644 (br, vs)	606 (sh, s)	570 (sh, w)	500 (w)	Dissoc.[c]	
	Bu^i	**18**	3252 (w)	675 (br, vs)	—	—	—	Dissoc.[c]	
	Pr^i	**19**	—	—	—	—	—	—	
	Bu^t	**20**	3246 (w)	587 (s)	558 (sh, w)	—	420 (s)	—	

[a] ν values in cm^{-1}; s, strong; m, medium; w, weak; br, broad; sh, shoulder; v, very. [b] ν_{N-H} of free amine. [c] The fragments are derived only from the dissociation into free trialkylaluminium and amine. [d] The fragments are derived from the corresponding dimeric amide, presumably formed on heating in the spectrometer.

fall in the activation energy of exchange found by NMR spectroscopy (see below). The change in N–H bond strength, however, is unlikely to be the sole determining factor of the difficulty of exchange.

With few exceptions, the frequencies of deformations in the adduct core do not vary significantly for different adducts with the same alkylaluminium moieties. However, the relative change in core frequencies with change in the alkylaluminium groups is not similar to the change in ν_{N-H} as the alkylamine groups change. Except for *iso*-butyl groups, which give results closer to methyl groups, there is only a general reduction in frequency with increasing bulk along the series (*i.e.* $Me \approx Bu^i > Et > Pr^i > Bu^t$). Thus as the steric bulk of the aluminium alkyl groups increases there is a concomitant decrease in the strength of bonds in the adduct core, including the adduct bond itself. This, clearly, will be another important factor in determining the stability of the complex.

Crystal structure

The structures of two adducts, $Me_3Al{\cdot}NHMe_2$ **1** and $Bu^t{}_3Al{\cdot}NHEt_2$ **10**, which have been determined are representative of molecules that are sterically unhindered and bulky, respectively. Crystal data are given in Table 2. Both structures consist of a central Al–N adduct bond with the aluminium atom surrounded by three alkyl groups in a flattened tetrahedron (the metal atom lying closest to the plane of its three co-ordinated carbon atoms), and the nitrogen atom of the amine in a distorted tetrahedron staggered relative to the aluminium alkyl groups (see Figs. 1 and 2). The relatively unhindered adduct **1** has a mirror plane through each molecule and so retains its molecular symmetry (C_m) in the crystal. The more bulky adduct **10** has lost its molecular symmetry due to crystal packing forces, which most noticeably affect the ethyl groups of the amine.

The effect of the difference in size of the alkyl groups on the bond lengths can be seen in Table 3, where it is clear that every bond length is significantly longer in adduct **10** than in comparative bonds in **1**, particularly around the aluminium where the difference is around 4%. This is in direct support of the trend found in the infrared spectra, which showed a decrease in the strength of bonds in the adduct core, including the adduct bond itself, as the steric bulk of the aluminium alkyl groups increased.

Table 2 Crystal data and structure refinement for compounds **1** and **10**

	1	**10**
Empirical formula	$C_5H_{16}AlN$	$C_{16}H_{37}AlN$
Formula weight	117.170	270.458
Crystal system	Monoclinic	Triclinic
Space group	$P2_1/m$	$P\bar{1}$
a/Å	6.230(1)	9.147(1)
b/Å	11.537(1)	9.857(1)
c/Å	6.723(1)	10.650(1)
α/°		91.31(2)
β/°	113.98(2)	97.42(2)
γ/°		92.59(2)
V/Å^3	441.51(0.12)	950.81(0.17)
Z	2	2
μ/cm^{-1}	1.24	0.72
Reflections collected	1211	4358
Independent reflections	1100	4158
No. observed reflections ($F_o > 3\sigma(F_o)$)	637	2099
Final R	0.0507	0.0418
Final R'	0.0442	0.0445

The bond angles show more specific differences; the aluminium alkyl group closest to the two amine alkyls is bent back dramatically in adduct **10** but insignificantly in **1**, compared to the other two alkyls, while the angles between the metal alkyl groups are all reduced by 1–2° in **1** compared to those in **10**. In addition, the irregular packing of the two ethyl groups on the amine in **10** is reflected in the angles of each relative to the adduct bond. The orientation in the ethyl groups of **10** around each N–C bond is also slightly different: the methylene protons of C4 are mutually *gauche* with the adduct bond, producing repulsion between C5 and C7 that places the methylene protons of C6 almost in eclipse with the adduct bond and C4. In both cases the methyl tail of the ethyl group is kept away from the bulky trialkylaluminium moiety.

The overall conclusions of this comparison, that increasing steric bulk produces bond lengthening, particularly in bonds with aluminium, and angle distortions to accommodate the

Table 3 Selected bond lengths (Å) and angles (°) of $Me_3Al{\cdot}NHMe_2$ **1** and $Bu^t_3Al{\cdot}NHEt_2$ **10**

Parameter	**1**	**10**
Al–N	2.000(5)	2.083(4)
Al–C(1)	1.973(6)	2.054(4)
Al–C(2)	1.965(5)	2.038(5)
Al–C(3)		2.040(4)
N–C(3)	1.476(4)	
N–C(4)		1.498(5)
N–C(6)		1.513(5)
N–Al–C(1)	103.4(3)	103.0(2)
N–Al–C(2)	102.9(2)	106.5(2)
N–Al–C(3)		103.8(2)
Al–N–C(3)	113.4(3)	
Al–N–C(4)		115.5(3)
Al–N–C(6)		113.4(3)

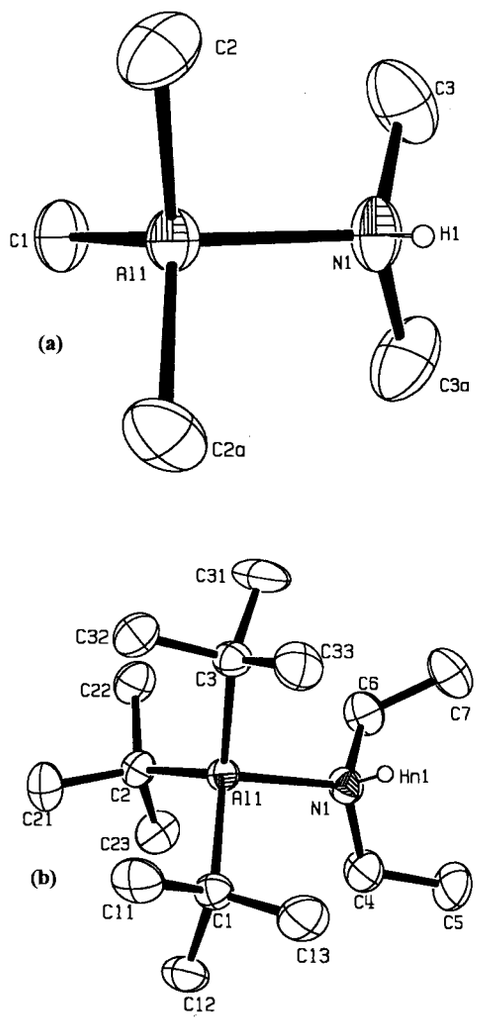

Fig. 1 Crystal structures of (a) $Me_3Al{\cdot}NHMe_2$ and (b) $Bu^t_3Al{\cdot}NHEt_2$.

larger groups, is in line with structural changes found in an extensive study of dimeric dialkylaluminium μ-dialkylamido compounds[10] and reflects the trend found here in the infrared data. Most specifically, the adduct bond length, hence strength, is sensitive to steric bulk.

Mass spectra

The mass spectra of the bulkier adducts, *i.e.* **5**, **10** and **15** which contain the Bu^t_3Al group and **14**–**20**, did not show any peaks corresponding to fragments containing both Al and N, *i.e.* only ion fragments of free trialkylaluminium and free amine were found. This is consistent with the expected weakening of the

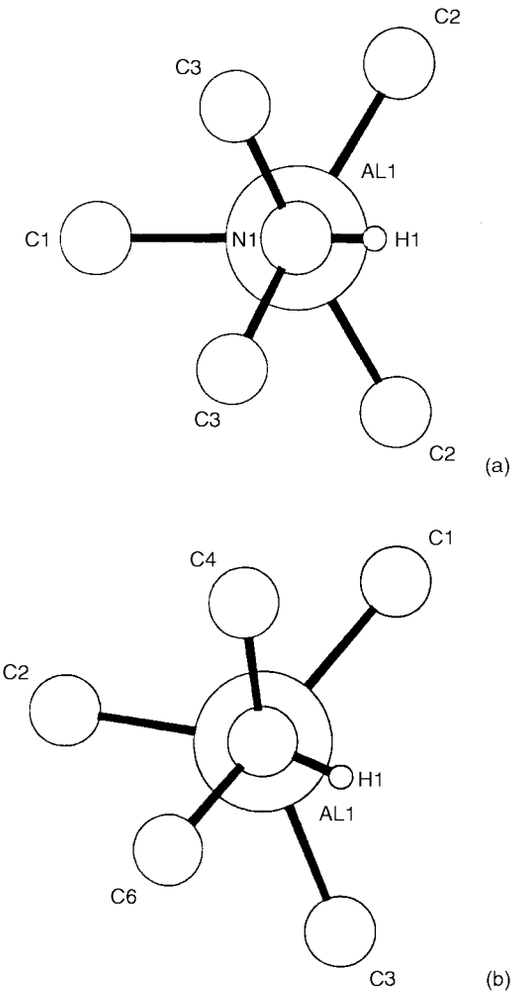

Fig. 2 Projection of the structures along the Al–N bond for (a) $Me_3Al{\cdot}NHMe_2$ and (b) $Bu^t_3Al{\cdot}NHEt_2$.

Al–N bond due to steric factors with increasing bulkiness of the R^1 and R^2 groups. All the other adducts, with their less bulky substituents, do show fragments $(M-R^1)^+$ which have the Al–N bond intact (Table 1); such species have previously been identified[11] in the mass spectra of $Me_3Al{\cdot}NHR^2_2$ (R^2 = Et, Pr^n, Pr^i, Bu^n or Bu^i). The intensity of the peak due to the $(M-R^1)^+$ fragment decreases as the steric bulk of the R^1 groups increases, with constant R^2, and this is further evidence to show that the steric interaction leads to a weakening of the Al–N bond.

^{1}H NMR spectra

In the range of compounds presented here, it is the protons of the R^2 groups which exhibited the most interesting effects in their ^{1}H NMR spectra. Adducts with the same amine moiety (the same R^2) are grouped together and summarised as follows.

Complexes with $R^2 = CH_3$. For these methyl groups only the expected doublet was found, and the vicinal coupling constant ($^3J_{NH-CH}$ = 7 Hz) was invariant with change in R^1. Only the methyl peak for adduct **3** showed broadening, however a well resolved doublet was obtained when the spectrum was measured at a lower temperature by 5 °C. These observations for **3** could only result from intermolecular exchange of the N*H* proton, presumably with traces of an excess of amine, since **3** had not been purified.

Complexes with $R^2 = CH_2CH_3$. The spectra of the methylene protons of diethylamine adducts are shown in Fig. 3. These constitute four types of spectra at ambient temperature as follows: (a) a single broad peak (**6**); (b) two broad peaks (**7**);

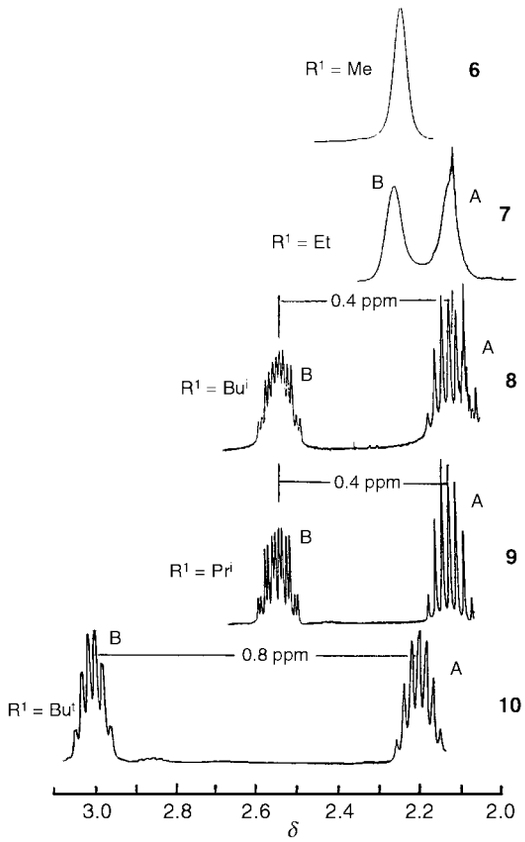

Fig. 3 Effect of change in the substituent R^1 upon the methylene proton region of the 250 MHz ^1H NMR spectra of the complexes $R^1{}_3Al{\cdot}NHEt_2$, measured at ambient temperature in C_6D_6 solution.

(c) two well resolved multiplets separated by $\Delta\delta = 0.4$ ppm (**8**, **9**); (d) as in (c), but with $\Delta\delta = 0.8$ ppm (**10**). The amino proton and an ethyl group constitute a AMM′X_3 spin system, the methylene protons within the ethyl group are prochiral and the two ethyl groups are equivalent. The well resolved methylene proton signals for **9** show coupling with the vicinal CH_3 protons ($J_{MX} = J_{M'X} = 7.0$ Hz), with the NH proton ($J_{AM} = 3.5$ and $J_{AM'} = 7.0$ Hz), and with each other ($J_{MM'} = 14.0$ Hz). The chemical shift separations of the methylene protons follow the order **10** > **9** ≈ **8** > **7** > **6**, which roughly follows the order of steric bulk of the substituents R^1 on aluminium, $Bu^t > Pr^i > Bu^i \approx Et > Me$. The spectra in Fig. 3 show that one of each methylene proton pair has a fairly constant chemical shift while the other shifts to high frequency with increasing bulk of R^1. The inequivalence of the methylene protons indicates that rotation of the ethyl groups around the N–C bond is increasingly hindered as the bulk of the Lewis acid increases, with a preferred conformation where the ethyl groups are bent away from the metal; this is consistent with the crystal structure of **10**.

The methylene proton multiplets for adduct **9** coalesce at elevated temperature showing that they are undergoing a chemical exchange process. At ambient temperature the slightly decreased resolution for **8** indicates somewhat faster exchange than for **9**. The spectrum for **7** shows the onset of coalescence while that for **6** indicates the exchange process is approaching the fast exchange regime. From the coalescence temperature of this exchange, approximate values for the free energy of activation ($\Delta G^{\ddagger}$) for the exchange process may be obtained in the manner described by Sandström[12] for the coalescence of a coupled AB type spectrum, eqns. (4) and (5) where $\Delta G^{\ddagger}$ is in kJ

$$\Delta G^{\ddagger} = 1.915 \times 10^{-2}\, T_c[10.319 + \log(T_c/k_c)] \qquad (4)$$

$$k_c = \pi\{0.5[(\delta\nu)^2 + 6J_{AB}{}^2]\}^{\frac{1}{2}} \qquad (5)$$

Table 4 NMR Parameters and the calculation of $\Delta G^{\ddagger}$

Adduct	J_{AB}/Hz	$\Delta\nu^a$/Hz	$T_c{}^a$/K	$k_c{}^b$/s^{-1}	$\Delta G^{\ddagger c}$/kJ mol^{-1}
6	14	32	228	104	47
7	14	55	338	144	69
8	14	98	358	230	72
9	14	105	370	245	74
10	14	202	332	455	65
14	0	16	335	36	72
15	0	16	297	36	69

[a] For ^1H observation at 250 MHz. [b] The rate coefficient at the coalescence temperature T_c. [c] Errors on $\Delta G^{\ddagger}$ are difficult to assess, but in comparing the $\Delta G^{\ddagger}$ values we believe an error *ca.* ±2 kJ mol^{-1} is reasonable.

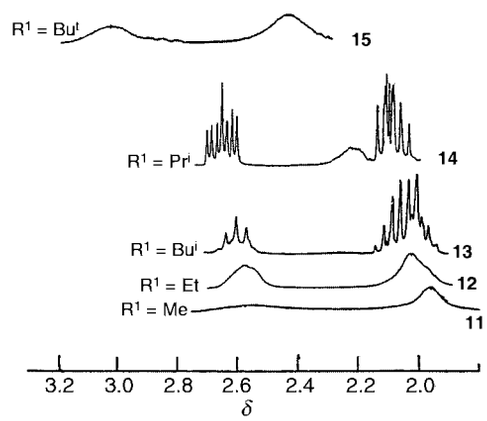

Fig. 4 Effect of change in the substituent R^1 upon the methylene proton region of the 250 MHz ^1H NMR spectra of the complexes $R^1{}_3Al{\cdot}NHBu^i{}_2$, measured at ambient temperature in C_6D_6 solution.

mol^{-1}, T_c is the coalescence temperature, k_c (s^{-1}) is the pseudo first order rate constant for the process at the coalescence temperature and $\delta\nu$ (Hz) is the limiting slow exchange chemical shift separation of the A and B resonances. The input data for the calculations and the results are given in Table 4. The $\Delta G^{\ddagger}$ values increase across the series **6** to **9**, with increasing bulk of the R^1 group, then decrease for **10** ($R^1 = Bu^t$). The significance of these values is discussed below.

Complexes with $R^2 = CH_2CH(CH_3)_2$. The appearance of the R^2 methylene proton signals, measured at 250 MHz and ambient temperature, is shown in Fig. 4. There is a strong similarity to the series of adducts **6** to **10** wherein $R^2 = Et$, in that the methylene protons are again prochiral and apparently undergoing a slow chemical exchange process. The chemical shift difference between the two resonances is fairly constant at *ca.* 0.6 ppm on changing R^1, and therefore qualitatively the $\Delta G^{\ddagger}$ values for the exchange process follow the order **11** ($R^1 = Me$) < **12** (Et) < **13** (Bu^i) < **14** (Pr^i) > **15** (Bu^t). This order is the same as found for the series **6** to **10**. The methyl groups of the Bu^i substituent also display prochirality and a similar qualitative order for exchange. The coalescence data for the methyl group exchange for **14** and **15** are given in Table 4, and the resulting $\Delta G^{\ddagger}$ values are quite similar to those for **9** and **10** respectively.

Complexes with $R^2 = CH(CH_3)_2$. The Me_3Al and Et_3Al complexes show the expected inequivalence of the methyl resonances. However the spectra of the complexes with the bulkier substituents ($R^1 = Bu^i$, Pr^i or Bu^t) do not show the inequivalence and at ambient temperature these resonances are in the fast exchange limit.

Mechanism of the exchange process. Two distinct mechanisms are possible to exchange the prochiral groups within R^2, involving dissociation of either the N–H or N–Al bond so that

the nitrogen may invert. Dissociation of the N–H bond is unlikely not only from the known chemistry of the aluminium alkyls, which are extremely aggressive deprotonating agents, but is also difficult to reconcile with the ^{1}H spectrum of $Me_3Al{\cdot}NHEt_2$ measured at a temperature above coalescence (+27 °C, in both d_6-benzene and d_8-toluene solutions). The methylene protons appear as an approximate 1:4:6:4:1 quintet (*J ca.* 6 Hz) indicating equal coupling to four protons, the vicinal methyl and N*H* groups, which is inconsistent with fast intermolecular exchange of the N*H* proton.

Dissociation of the Al–N bond, on the other hand, is easy to demonstrate in exchange reactions like (2). For example, when approximately equimolar amounts of the adducts **1** ($R^1 = R^2 =$ Me) and **8** ($R^1 = Bu^i$, $R^2 =$ Et) are mixed the resulting ^{1}H NMR spectrum shows distinctive resonances from both **1** and **8**, as well as from **3** ($R^1 = Bu^i$, $R^2 =$ Me) and from **6** ($R^1 =$ Me, $R^2 =$ Et).

With this model for exchange, it is possible to address the activation parameters presented in Table 4 for complexes **6**–**10** (diethylamine adducts with a series of trialkylaluminiums) and **14** and **15** (isobutylamine adducts). The infrared data have shown that in general a change in aluminium alkyl group has a more marked effect on the bonding, including the adduct bond, than changing the amine has. Thus a comparison of the free energies is best made for a constant aluminium alkyl group. In the case of the tri-*tert*-butylaluminium adducts, **10** and **15**, two different free energies have been obtained at two different temperatures. Assuming the difference in amine alkyl is not a factor (both are connected to nitrogen by a methylene unit), the change in free energy must then be due to the entropy contribution. A drop of 3.8 kJ mol^{-1} over a rise in temperature of 35 °C indicates an entropy of -108 JK^{-1} mol^{-1} which is in accord with the dissociative mechanism of Scheme 1 and this suggests

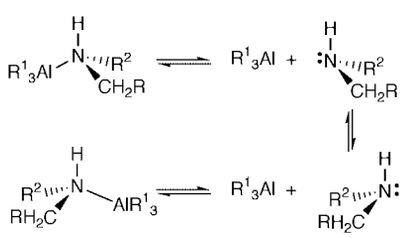

Scheme 1

an adduct bond strength of approximately 100 kJ mol^{-1} in these tri-*tert*-butylaluminium adducts.

The comparison of tri-*iso*-propylaluminium adducts **9** and **14** is not in accord with the mechanism of Scheme 1. A positive entropy of 57 J K^{-1} mol^{-1} suggests an associative process and an enthalpy of 53 kJ mol^{-1} is too low for a simple breaking of an adduct bond such as this. As already mentioned, the amine must be dissociated to invert, so a bimolecular amine exchange, where free amine attacks the aluminium atom in an adduct molecule to displace the existing amine, is indicated. This is in accord with a positive entropy of activation and with amine exchange in a mixture of adducts **1** and **8**, as well as the more facile exchange observed in **3** in the presence of a trace excess of amine. The thermodynamic parameters obtained from this exchange therefore represent the cumulative effect of two mechanisms, the dissociation of the adduct bond (an initiation of a chain of reactions) and then bimolecular exchange of free amine with an adduct (which propagates the chain). Reaction of free amine with free aluminium trialkyl will terminate the reaction chain. Exchange can thus be promoted either when steric compression around the adduct bond is great, because this weakens the bond and so increases initiation steps, or when the steric bulk around the aluminium is low, because this will facilitate attack by free amine, thus increasing the number of propagation steps before termination. Adducts which have neither a great driving force to dissociate nor an easy amine-exchange intermediate will therefore have a higher free energy of exchange. The results in Table 4 indicate that only in the tri-*tert*-butylaluminium adducts the increasing steric crowding around the aluminium significantly weakens the adduct bond and thus promotes dissociation; with small alkyls it just becomes more difficult to form bimolecular exchange intermediates.

Conclusion

The analysis of the ^{1}H NMR data shows that exchange in the environments of the diastereotopic methylene protons (and methyl groups) of the amine moieties in the complexes is due to a dissociative mechanism with breaking of the Al–N bond, not of the N–H bond. Free amine molecules thus produced can go on to react with further adduct molecules in an associative exchange mechanism (either concerted or addition-elimination) to propagate amine exchange. This will end in a termination step where free amine reacts with free trialkylaluminium. The trend in the activation parameter for the exchange process for complexes **6**–**10**, $R^1{}_3Al{\cdot}NHMe_2$ is an increase across the series $R^1 =$ Me < Et, Bu^i < Pr^i, showing increased difficulty of propagation as groups around the aluminium become more bulky. This is followed by a decrease for Bu^t, showing a marked increase in adduct dissociations due to steric compression across the adduct bond.

The trend in the NH stretching frequency mirrors the trend in the exchange energies; the greatest weakening of the NH bond occurs with very small or very large aluminium alkyl groups. The weakening when alkyl groups are small will be marked because of the loss of electron density from the nitrogen into the adduct bond, reducing the polarity of the NH bond and so weakening the ionic contribution to the bond strength. Larger alkyl groups on the aluminium will supply more electron density to the metal, thus lessening the pull of electron density from the amine and lessening the NH bond weakening, until a point is reached when the bulk around the aluminium starts pushing into the amine. This will then directly interfere with and weaken the NH bond. A continual rise in the steric compression around the aluminium is indicated in the collective rise of the aluminium-related stretches with increasing group size and shown directly in the crystal structures.

Experimental

All compounds were manipulated under dry nitrogen using a vacuum line, glove-box and Schlenk-style apparatus. Proton NMR spectra were obtained using Bruker AM-250 and AMX-400 spectrometers, with samples in dried deuteriobenzene and deuteriotoluene solutions sealed into 5 mm o.d. tubes. Infrared spectra (neat and Nujol mulls placed between CsI plates) in the 4000–200 cm^{-1} range were obtained using a Perkin-Elmer FT1720X spectrophotometer and mass spectra using an AEI MS902 spectrometer operating at 70 eV (*ca.* 1.12×10^{-17} J). The analyses (C, H and N) were obtained from the Microanalytical Service of University College London.

For structure determination, under a nitrogen atmosphere, a suitable single crystal was selected, attached to a glass fibre by using silicon grease then mounted inside a 0.7 mm diameter glass capillary which was flame sealed. The intensity data were collected on a CAD4 diffractometer with Mo-Kα radiation (λ 0.71069 Å) using ω–2θ scans at 290 K. The unit-cell parameters were determined by a least-squares refinement on diffractometer angles for 25 automatically centered reflections ($9 \leq \theta \leq 12$ and $10 \leq \theta \leq 13°$). The structures were solved by direct methods using the SHELXS[13] program package, and refined anisotropically (non-H atoms) by full-matrix least squares on *F*, using the SHELXS 80[14] program package. All H atom positions were found from subsequent difference maps,

Table 5 Summary of the experimental conditions for the synthesis of the adducts $R^1_3Al{\cdot}NHR^2_2$

Compound	Reagents		Reaction		Product	Purification[a]	Yield (%)
	R^1_3Al/mmol	NHR^2_2/mmol	Temperature/°C	Time/h			
1	33	38	−30	1	white solid	Sublime; 25 °C	87
2	61	67	−30	2	clear liquid	Distil; 50 °C	82
3	29	34	−20	6	clear liquid	Crude	100
4	24	44	−40	48	clear liquid	Distil; 85 °C	77
5	19	25	−20	12	white solid	Sublime; 80 °C	91
6	93	116	25	1	clear liquid	Distil; 50 °C	96
7	67	77	25	4	clear liquid	Distil; 100 °C	92
8	40	48	0	12	clear liquid	Distil; 85 °C	80
9	38	80	25	23	clear liquid	Distil; 80 °C	89
10	28	33	25	15	white solid	Sublime; 65 °C	85
11	111	126	25	1	clear liquid	Distil; 80 °C	95
12	33	40	−20	1	clear liquid	Crude	100
13	19	29	−20	1	clear liquid	Crude	100
14	24	27	25	48	clear liquid	Distil; 100 °C	87
15	29	40	25	2	white solid	Sublime; 100 °C	93
16	112	143	25	1	clear liquid	Distil; 45 °C	93
17	96	107	25	1	clear liquid	Distil; 80 °C	91
18	43	44	−20	1	clear liquid	Crude	100
19	8	11	−20	48	white solid	Crude[b]	100
20	10	14	−20	1	white solid	Crude	100

[a] At 10^{-2} mbar. [b] Begins to decompose at room temperature.

Table 6 Analytical data[a] for adducts $R^1_3Al{\cdot}NHR^2_2$

Compound	C	H	N
1	50.3(51.2)	14.3(13.8)	12.3(12.0)
2	65.3(60.4)	10.6(13.8)	8.4(8.8)
3			
4	67.8(65.7)	13.6(13.9)	7.0(6.9)
5	68.5(69.1)	14.3(14.1)	5.9(5.8)
6	58.2(57.9)	13.7(13.8)	9.4(9.6)
7	63.0(64.2)	14.4(14.0)	7.2(7.5)
8	70.5(70.8)	14.3(14.1)	5.2(5.2)
9	68.1(68.1)	13.9(14.0)	5.8(6.1)
10	71.2(70.8)	13.5(14.1)	5.6(5.2)
11	64.8(65.6)	14.4(14.0)	6.8(7.0)
12	67.7(69.1)	13.6(14.1)	5.6(5.8)
13	72.5(73.3)	13.9(14.2)	4.6(4.3)
14	70.2(70.0)	14.1(15.9)	4.7(4.8)
15	72.9(73.3)	13.7(14.2)	4.8(4.2)
16	61.9(62.3)	13.5(14.0)	7.9(8.1)
17	65.4(66.9)	13.0(14.1)	6.1(6.5)
18	70.3(72.2)	14.1(14.0)	4.6(4.7)
19			
20	67.9(72.2)	13.4(14.0)	3.3(4.7)

[a] Values as %, calculated values in parentheses.

except the methyl hydrogens of compound **1**, which were fixed using the SHELX facility for a riding model. The program ORTEP 3[15] was used for drawing the molecules.

CCDC reference 186/1627.

Table 5 summarises the experimental conditions of synthesis. All aluminium alkyls, R^1_3Al, were used as solutions; R^1 = Me, Et, Bu^i or Bu^t in light petroleum, bp 40–60 °C (Aldrich), $R^1 = Pr^i$ (freshly prepared) in diethyl ether. The amines NHR^2_2 (Aldrich) where R^2 = Et, Bu^i or Pr^i were used neat; $NHMe_2$ was used as a solution in light petroleum because of its volatility. Low temperatures were often required during synthesis, either to combat the volatility of $NHMe_2$ or to prevent adduct decomposition to the amide caused by exothermic adduct formation. The adducts were purified where possible by distillation or sublimation *in vacuo*. Thermal decomposition to the amide (for **3**, **11**, **12**) or a yellow oil (for **18**, **19**, **20**) prevented purification of some compounds; despite this, very clean ^{1}H NMR spectra were obtained from the crude products, which were therefore used unpurified.

Table 6 gives the elemental analysis data for the adducts. The remaining data, *viz.* those obtained from infrared, ^{1}H NMR and mass spectra, are available as SUP 57633.

Acknowledgements

One of us (I. A. M.) would like to thank the Brazilian Research Council (CNPq) and the Research Centre of the Brazilian Telecom (CPqD-Telebras) for financial support. We also thank Mr P. Cook for the measurement of the mass spectra.

References

1 T. Mole and E. A. Jeffery, *Organoaluminium Compounds*, Elsevier, Amsterdam, 1972, p. 106.
2 T. Mole, *Aust. J. Chem.*, 1963, **16**, 801; 1965, **18**, 1183.
3 D. M. Frigo, P. J. Reuvers, D. C. Bradley, H. Chudzynska, H. A. Meinema, J. G. Kraaijkamp and K.Timmer, *Chem. Mater.*, 1991, **3**, 1097.
4 K. Gosling and R. E. Bowen, *J. Chem. Soc.*, *Dalton Trans.*, 1974, 1961.
5 K. Haage, K. B. Starowieski and A. Chwojnowski, *J. Organomet. Chem.*, 1979, **174**, 149.
6 F. C. Sauls, L. V. Interrante and Z. Jiang, *Inorg. Chem.*, 1990, **29**, 2989.
7 C. N. McMahon, S. G. Bott and A. R. Barron, *J. Chem. Soc.*, *Dalton Trans.*, 1997, 3129.
8 N. R. Fetter, B. Bartocha, F. E. Brinckman, Jr. and D. W. Moore, *Can. J. Chem.*, 1963, **41**, 1359; J. Chatt, L. A. Duncanson and L. M. Venanzi, *J. Chem. Soc.*, 1956, 2712.
9 L. K. Krannich, C. L. Watkins and D. K. Srivastava, *Polyhedron*, 1990, **9**, 289.
10 D. C. Bradley, I. S. Harding, I. A. Maia and M. Motevalli, *J. Chem. Soc.*, *Dalton Trans.*, 1997, 2969.
11 K. H. Thiele, H. K. Müller and W. Brüser, *Z. Anorg. Chem.*, 1966, **345**, 194.
12 J. Sandström, *Dynamic NMR Spectroscopy*, Academic Press, London, 1982, pp. 84, 96.
13 G. M. Sheldrick, SHELXS 86, *Acta Crystallogr.*, *Sect. A*, 1990, **46**, 467.
14 G. M. Sheldrick, SHELXS 80, University of Göttingen, 1980.
15 L. J. J. Farrugia, ORTEP 3 for Windows, *J. Appl. Crystallogr.*, 1997, **30**, 565.

Paper 9/02973G